Dynamic Mechanical Properties of Oil Palm Microfibril-Reinforced Natural Rubber Composites

Shaji Joseph,[1] Sreekumar P. Appukuttan,[2] Jose M. Kenny,[3] Debora Puglia,[3] Sabu Thomas,[4] Kuruvilla Joseph[5]

[1]*Department of Chemistry, St. Berchmans' College, Kottayam, Kerala 686 101, India*
[2]*Polymer Technology Laboratory, National Institute of Technology Calicut, Calicut, Kerala 673 601, India*
[3]*University of Perugia, Loc. Pentima Bassa, 21 - 05100 Terni, Italy*
[4]*School of Chemical Sciences, Mahatma Gandhi University, Kottayam, Kerala 686 560, India*
[5]*Department of Chemistry, Indian Institute of Space Science and Technology (IIST), Trivandrum, Kerala, India*

Received 26 February 2008; accepted 19 October 2008
DOI 10.1002/app.30960
Published online 29 March 2010 in Wiley InterScience (www.interscience.wiley.com).

ABSTRACT: The dynamic mechanical properties of macro and microfibers of oil palm-reinforced natural rubber (NR) composites were investigated as a function of fiber content, temperature, treatment, and frequency. By the incorporation of macrofiber to NR, the storage modulus (E') value increases while the damping factor (tan δ) shifts toward higher temperature region. As the fiber content increases the damping nature of the composite decreases because of the increased stiffness imparted by the natural fibers. By using the steam explosion method, the microfibrils were separated from the oil palm fibers. These fibers were subjected to treatments such as mercerization, benzoylation, and silane treatment. Resorcinol-hexamethylenetetramine-hydrated silica was also used as bonding agent to increase the fiber/matrix adhesion. The storage modulus value of untreated and treated microfibril-reinforced composites was higher than that of macrofiber-reinforced composites. The T_g value obtained for this microfibril-reinforced composites were slightly higher than that of macrofiber-reinforced composites. The activation energy for the relaxation processes in different composites was also calculated. The morphological studies using scanning electron microscopy of tensile fracture surfaces of treated and untreated composites indicated better fiber/matrix adhesion in the case of treated microfibril-reinforced composites. Finally, attempts were made to correlate the experimental dynamic properties with the theoretical predictions. © 2010 Wiley Periodicals, Inc. J Appl Polym Sci 117: 1298–1308, 2010

Key words: oil palm microfibrils; microcomposites; steam explosion; dynamic mechanical properties

INTRODUCTION

In the recent years a number of industrial sectors, including automotive, building, and aerospace industries, have shown immense interest to natural fibers in order to replace glass fibers as reinforcement in composites for structural applications.[1] Agro fiber-reinforced composites show good mechanical properties and cause less abrasive wear during the process.[2] The natural fibers are immensely used in automotive components such as door trims, instrument panels, and headrests and no sharp splintering occurs during collision.[3,4] The inexpensive and lightweight composite materials from these renewable sources have lower material density, thus showing improved fuel efficiency if applied in the transport sector.[5,6] Many natural fibers have been successfully used for reinforcing elastomers in the production of low-cost composite materials.[7] The incorporation of short fibers in rubber imparts increased strength and stiffness to the matrixes.[8] It is also possible to achieve reduction of cost of the molding compound, improved process ability, and good physical, chemical, and electrical properties.[9]

Dynamic mechanical analysis (DMA) has been widely employed for determining the interfacial characteristics of heterogeneous polymeric systems. It gives us an understanding regarding the viscoelastic behavior of molten polymeric materials and the glass transition region of the composites.[10] Storage modulus gives an insight into the stiffness behavior and load-bearing capability of composite material.[11] Tan δ is related to the degree of molecular mobility in the polymeric material. The glass transition temperature (T_g) can be defined as the maximum of the transitions in the loss modulus or tan δ curve at low frequencies.[12]

Many researchers examined the dynamic mechanical behavior of natural fiber-reinforced polymeric composites. Jacob et al.[13] studied the dynamic behavior of sisal/oil palm hybrid fiber-reinforced

Correspondence to: K. Joseph (kuruvillajoseph@sancharnet.in).

natural rubber (NR) composites. The storage modulus was found to increase with weight fraction of fiber. In the case of chemically modified fibers, storage modulus and loss modulus were found to vary as a function of the fiber surface modification. Geethamma et al.[14] investigated the viscoelastic properties of short coir fiber-reinforced NR composites. It was found that the composite with poor interfacial bonding tend to dissipate more energy than that with good interfacial bonding. DMA of soy protein-reinforced styrene–butadiene rubber (SBR) composites were studied by Jong.[15] The addition of soy protein to the rubber composites generated a significant effect. Physicomechanical properties of α-cellulose-filled SBR composites have been studied by Haghighat et al.[16] Martins and Mattoso[17] studied the viscoelastic characteristics of sisal fiber-reinforced tire rubber composites and showed that mercerization/acetylation treatment increases the dynamic mechanical properties. The results showed that these composites are potential for nonstructural applications. The DMA of fly ash-filled NR modified with cardanol derivatives was carried out by Menon et al.[18] The stabilizing effect of lignin filler on NR was examined by Kosikova et al.[19] by using DMA. It was observed that the dynamic mechanical properties of NR vulcanisates were considerably improved by the addition of lignin. The mechanical and dynamic mechanical properties of rice husk ash-filled NR compounds were studied by Da Costa et al.[20] The T_g values of filled rubber vulcanisates shifted to higher temperatures, showing the presence of crosslinks, which restrict the mobility of polymer chains. The interactions between fillers and rubber phase also account for the higher properties.

A number of studies as aforementioned have been reported on the dynamic mechanical behavior of natural fiber-reinforced polymer matrix composites. It is important to mention that the studies on cellulose microfibrils-reinforced composites are very few. Therefore, there is every need to study the microfibril-reinforced polymer composites. The high aspect ratio and surface area of microfibrils are effective in reinforcing the rubber matrix. For successive applications, the stiffness and strength have to satisfy the requirements of low temperatures of about −20 to 100°C. In this article we present the dynamic mechanical properties of untreated oil palm macro/microfiber-reinforced NR composites, with special reference to fiber loading. The effects of fiber/fibrils treatment on the dynamic properties of microfibrils-reinforced NR composites were studied in detail. The effect of frequency on the dynamic properties of the composites was evaluated. The properties were correlated with the morphology of the fibers.

EXPERIMENTS

Materials

Oil palm fiber was obtained from Oil Palm India Ltd., Kottayam, Kerala, India. The properties of oil palm empty fruit bunch fiber are presented in Table I. The empty fruit bunch was subjected to wetting. Then the fibers were cleaned, washed, and dried in an air oven at 80°C for 5 h and kept in polythene bags to prevent moisture absorption. NR used for the study was ISNR-5 (light color) grade obtained from the Rubber Research Institute of India, Kottayam. The silane-coupling agent was obtained from Sigma-Aldrich, India. All other rubber ingredients, such as vulcanizing agents, accelerators, and activators, were chemically pure grade and obtained from Scientific and Industrial Supplies Corporation, Mumbai, India.

Preparation of microfibrils—Steam explosion method

Steam explosion (STEX) method is used as pretreatment to separate lignin, hemicellulose, wax, and pectin from lignocelluloses biomass. The high temperature of STEX process softens the material, and the mechanical action during high pressure results in microfibril separation. In plant cell wall, lignin and hemicellulose forms coating over cellulose and thus the matrix cannot easily flow through the fibers when composites are prepared. So a pretreatment is required to improve the moisture resistance power and to enhance the surface interactions. The main objective of microfibrillation is to remove the lignin and other noncellulosic materials including hemicellulose, pectin, waxes, etc., through STEX method followed by a chemical treatment for purifying the cellulose residue.

The oil palm empty fruit bunch fibers were cut into small pieces and put in an autoclave with 2% NaOH solution. High pressure and steam were produced in the autoclave, in which the fiber was kept in a Teflon case with a strong steel outer covering. About 50 g of fiber can be put into it at a time. The high temperature and pressure developed inside the case helps to individualize the fiber. Then the samples were kept in the autoclave at different hours (1, 2, and 5 h). After the required duration, the samples were taken out of the vessel and then cooled to room temperature. The treated samples were then used for the bleaching action.

A schematic representation of the microfibril preparation is given in Figure 1. The steam-exploded fibers were washed with distilled water at room temperature and soluble impurities were removed by filtration. The water-insoluble residue was then bleached in a magnetic stirrer with solutions of

TABLE I
Physical and Mechanical Properties of Oil Palm Macrofiber

Properties	Oil palm macrofiber
Diameter (μm)	150–500
Density (g/cm^3)	1.51
Elastic modulus (GPa)	3.2
Tensile strength (MPa)	240–550
Elongation at break (%)	14
Microfibrillar angle (°)	46
Cellulose (wt %)	65
Lignin (wt %)	19
Hemi cellulose (wt %)	–
Ash (wt %)	2

sodium hypochlorite (NaOCl), NaOH, and CH_3COOH (at specific proportion) at a temperature of 80°C for 1 h. The residue was washed with water and the process was repeated till a white crystalline product was seen. The white product was then washed with water and dried. The dried cellulose was then disintegrated for 20 min in a mechanical grinder.

Microfibril surface modification

Mercerization

The microfibrils were taken in a stainless steel vessel. A 5% solution of NaOH was added into the vessel, stirred well, and kept for 1 h with stirring, and then the microfibrils were washed with distilled water containing little acetic acid and dried.

Silane treatment

Vinyl tris (2-ethoxy methoxy silane) was used as coupling agent for the treatment. The respective (0.4%) silane was prepared by mixing with ethanol/water mixture in the ratio 6 : 4 and was allowed to stand for 1 h. The pH of the solution was maintained between 3.5 and 4 with the addition of acetic acid. Oil palm microfibrils were immersed in NaOH solution, then dipped in the silane solution, stirred well, and allowed to stand for 1.5 h. The ethanol/water mixture was drained out and the fibers were dried in air and then in an oven at 70°C until the fibers were completely dry.

Benzoyl chloride treatment (benzoylation)

About 35 g of microfibril were soaked in NaOH for 1 h, filtered, and washed with water. The treated microfibrils were agitated well with 50 mL benzoyl chloride. The mixture was keep for 15 min, washed with water, and dried. The isolated microfibrils was soaked in ethanol for 1 h to remove the unreacted benzoyl chloride and finally washed with water and dried.

Preparation of microcomposites with well-dispersed cellulose microfibrils

The formulation of the mixes is given in Tables II and III. The composite materials were prepared in a laboratory two-roll open mixing mill (150 × 300 mm^2). The nip gap, mill roll speed ratio (1 : 1.25), time, temperature of mixing, number of passes, and sequence of addition of ingredients during mixing were kept the same for all mixes. NR was initially masticated on the mill for 2 min and then the additives were added. The microfibrils were added at the end of the compounding process. Then the samples were milled for 15 min to confirm uniform microfibril

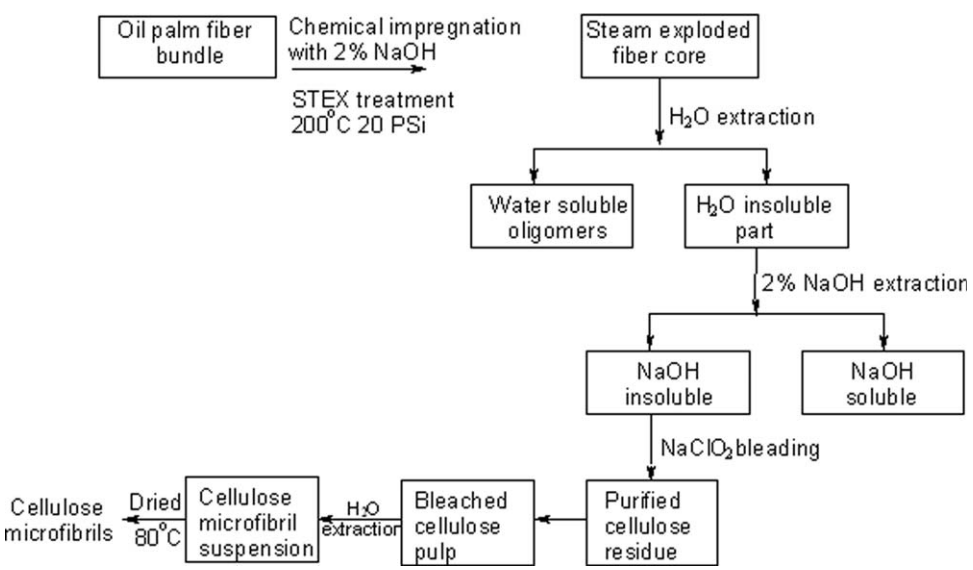

Figure 1 Schematic representation of the preparation of cellulose microfibrils.

TABLE II
Formulation of the Mixes of Macrofiber-Reinforced Composites

Ingredients[a]	NR	NRF10	NRF20	NRF30
Natural rubber	100	100	100	100
ZnO	5.0	5.0	5.0	5.0
Stearic acid	1.5	1.5	1.5	1.5
TDQ[b]	1.0	1.0	1.0	1.0
CBS[c]	0.6	0.6	0.6	0.6
Sulfur	2.5	2.5	2.5	2.5
Oil palm fiber[d] content	–	10.0	20.0	30.0

[a] Parts per hundred rubber (phr).
[b] 2,2,4-Trimethyl 1,2-dihydroxy quinoline.
[c] *N*-cyclohexyl-2-benzothiazyl sulfenamide.
[d] Fiber length = 6 mm.

distribution. The rolling direction was kept constant because of its importance for microfibril orientation.

Dynamic mechanical analysis

The dynamic mechanical behavior of oil palm fiber composites was studied by using a rheometer of model ARES N2 Rheometric Scientific. The testing temperature ranged from −100 to 100°C and the experiment was carried out at frequencies 0.1, 1, 10 Hz at 5°C/min.

FTIR analysis

The modified fiber surface was characterized by IR spectroscopy. A Shimadzu IR-470 spectrophotometer was used for the IR study. Powdered fiber palletized with potassium bromide was used for recording the spectra.

Scanning electron micrograph analysis

The fracture morphology of the composites was observed by means of scanning electron microscopy (SEM). SEM studies were conducted using Zeiss FESEM supra 25, to analyze the fracture behavior of the composites. The fracture ends of the tensile specimens of the composites were mounted on aluminum stubs and gold coated to avoid electrical charging during examination. The tensile fractography and hence interfacial adhesion between the matrix and fiber were examined by SEM.

RESULTS AND DISCUSSION

Characterization of microfibers

The SEM of raw fibers and STEX microfibrils are shown in Figure 2(a,b), respectively. SEM studies inferred that the diameters of macrofibers (194–279 μm) are higher than microfibers (5–20 μm). After STEX the microfibrils showed three major changes: (a) an increase in effective surface area available for contact with wet matrix due to fiber bundle fibrillation; (b) fiber porosity increases because of lignin redistribution and the surface is changed to rough; (c) porosity is caused by the hydrolysis and removal of hemicellulose. The aspect ratio of the fibrils is high (100–125) with relatively good orientation as evident from the micrograph. The diameter of the macrofiber is drastically reduced from 194 to 5 μm depending upon the treatment.

The FTIR spectra of the macro and microfibers are given in Figure 3. The characteristic feature of the IR spectrum of oil palm fiber is due to the lignin and hemicellulose components that exist in fibers. From the IR spectrum the following peaks have been observed. The strong broad peak at 3300–3400 cm^{-1} in the oil palm fiber is the characteristic hydrogen bonded —OH stretching vibrations. The strong peak at 2900 cm^{-1} is due to the —CH stretching vibrations. The peak at 1730 cm^{-1} is the characteristic band for carbonyl stretching. The important change expected here is the removal of hydrogen bonding in the network structure. This was evident from the increased intensity of the —OH peaks at 3300 cm^{-1}. Also upon microfibrillation a peak at 1735 cm^{-1} assigned to C=O stretching vibration of carboxylic

TABLE III
Formulation of the Mixes of Microfiber-Reinforced Composites

Ingredients	NRM10	NRM20	NRM30	NRMB30	NRMS30	NRMH30
Natural rubber	100	100	100	100	100	100
ZnO	5.0	5.0	5.0	5.0	5.0	5.0
Stearic acid	1.5	1.5	1.5	1.5	1.5	1.5
Resorcinol	–	–	–	–	–	7.5
Hexa	–	–	–	–	–	4.8
silica	–	–	–	–	–	2
TDQ	1.0	1.0	1.0	1.0	1.0	1.0
CBS	0.6	0.6	0.6	0.6	0.6	0.6
Sulfur	2.5	2.5	2.5	2.5	2.5	2.5
Oil palm microfibrils	10.0	20.0	30.0	30.0	30.0	30.0
Treatments	5% NaOH, 1 h	5% NaOH, 1 h	5% NaOH, 1 h	Benzoylation	Silane	HRH

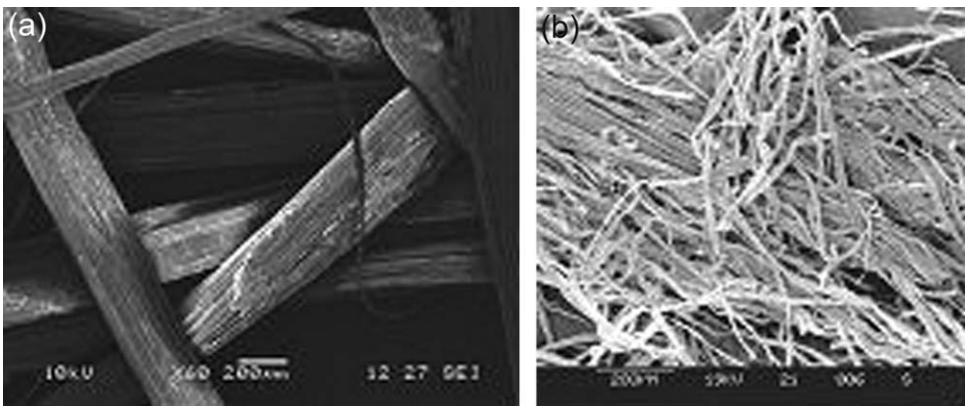

Figure 2 SEM images of (a) oil palm macrofibers and (b) steam-exploded oil palm microfibers.

acid or ester in the spectrum of the raw fiber disappeared. This was due to the fact that a substantial amount of uranic acid, a constituent of hemicellulose (xylan), was removed from the fiber, resulting in the disappearance of the peak. The band near 1400 cm^{-1} is assigned to the —CH_2 symmetrical deformation. The band at 1370, 1330, and 1310 cm^{-1} are due to —CH deformation, —OH in plane bending, and —CH_2 wagging, respectively. The band near 1245 cm^{-1} is due to the —C—O—C— bond in the cellulose chain. The peak near 900 cm^{-1} is characteristic of β linkages.

Effects of macrofiber on dynamic properties

Storage modulus

The variation of storage modulus with temperature can be seen in Figure 4. A clear understanding of storage modulus vs. temperature curve provides valuable information about the stiffness of a material, degree of cross linking, and fiber/matrix interfacial bonding. It can be seen that storage modulus increases with the increasing oil palm fiber content when compared with the matrix. In all the composites, *E′* decreased with the increase in temperature and the significant fall is observed in the region between −60 and –40°C. In the glassy region the components are in a frozen state and are highly immobile. So the storage modulus value does not show much variation. When temperature increases the substance becomes more mobile and loses its close packing arrangement, and as a result the modulus decreases. But at higher temperature the modulus values vary as a function of fiber content and are maximum for the composites having fiber loading of 30 phr (NRF30). In composites, the greater degree of stress transfer at the interface is controlled by the fiber/matrix interaction. The NR comprising only the rubber phase gives the material more flexible character resulting in a low degree of stiffness of material and hence low storage modulus. At low fiber loading the matrix is not restrained by enough fibers and highly localized strains occur in the matrix at low stresses, causing the bond between the matrix and fiber to break, leaving the matrix diluted by nonreinforcing debonded fibers. As the fiber concentration increases (30 phr), the stress is more evenly distributed and the composite strength and modulus increases.

Damping factor

Tan δ is a damping term that can be related to the impact resistance of a material. As the damping peak occurs in the region of glass transition where the material changes from a rigid to a more elastic state, it is associated with the movement of small groups and chains of molecules within the polymer structure, all of which are initially frozen. Therefore, higher the tan δ peak value, greater is the degree of molecular mobility.[21]

The variation of tan δ of the composites as a function of temperature is given in Figure 5. The gum

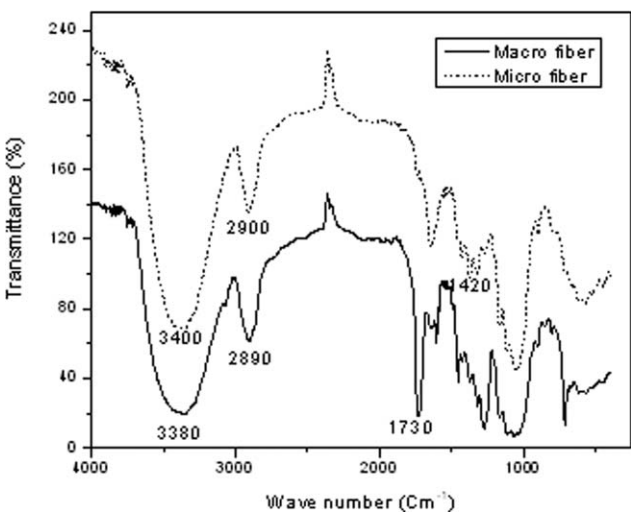

Figure 3 FTIR spectra of oil palm macro and microfibers.

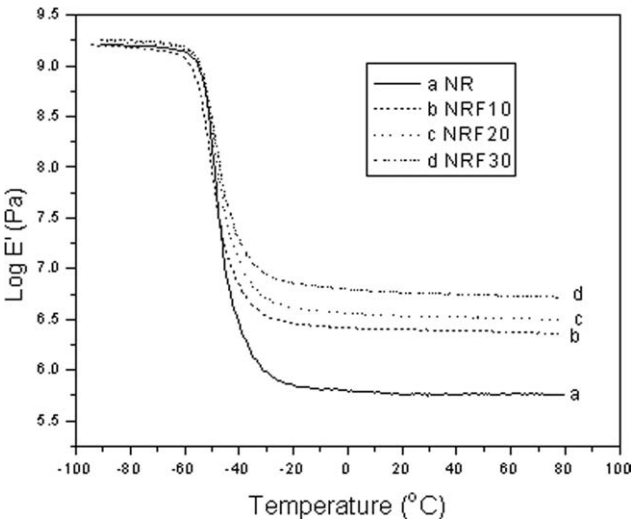

Figure 4 Storage modulus vs. temperature curve of untreated oil palm macrofiber/NR composites having various fiber content.

compound has the highest tan δ value, indicating a large degree of molecular mobility. The damping peak of the composites showed a decreased peak height with increased filler loading and is clearly shown in Table IV. This is because the fibers carry a greater extent of stress and allow only a small part of it to strain the interface. Therefore, lesser energy dissipation will occur in the composite, where matrix to fiber interaction is strong, whereas greater energy dissipation will occur in the rubber matrix. Incorporation of fibers acted as barriers to the mobility of rubber chains, leading to lower flexibility, lower degrees of molecular motion, and hence lower damping characteristics. Lesser the interfacial adhesion between fiber and matrix, greater will be the damping.[22] As seen in Figure 5, at higher fiber loading (30 phr), interface between fiber and rubber matrix is stronger, chain flexibility is arrested, and T_g shifts slightly toward higher temperature region. Therefore, we can conclude that the presence of natural fibers decreases the damping of the composites.[23]

Effects of microfiber on dynamic properties

All plant fiber consists of microfibrillated cellulose whose diameter is about 2–10 μm with a high aspect ratio. Cellulose microfibrils-reinforced rubber composites also have extremely excellent mechanical properties because of its crystal structure.[5] Dufresne et al.[24] explained that nanocomposite materials from microcrystalline starch-reinforced thermoplastic matrix have good dynamic mechanical properties. Agnes et al.[25] indicated that chemical modification of fibers has profound influence on the dynamic mechanical properties of composites. The cellulose microfibrils prepared by STEX (alkali treatment) have improved surface characteristic properties, because hemicellulose, lignin, pectin, and other impurities have been removed. Thus, the cellulose microfibrils become rough and have a good surface topography. The extent of these microfilaments in fibril network and the adhesion properties of the matrix with the microfibrils are the major factors contributing to the overall dynamic properties of the composites.

Storage modulus

Figure 6 represents the variation of storage modulus against temperature of microfibril-reinforced rubber composites. It can be seen that E' increases moderately with increasing microfibril content at all temperatures when compared with the gum. During continuous mercerization of fibers by STEX, the fibrils become more rough and the moisture absorbing capacity of fibrils are reduced, leading to improved wetting which produces strong interfacial adhesion with the rubber matrix and gives rise to a much stiffer composite with higher modulus.[26] The increased surface area of microfibrils results in increased crosslinks with the rubber matrix, which contributes to higher E' values. In the case of macrofibers due to the presence of lignin, hemicellulose, etc., fiber/matrix interaction is weak, thus resulting in lower E' values.

Damping factor

The variation of tan δ with temperature is given in Figure 7. As seen in this figure, microfibril (30 phr)-reinforced rubber composite possesses lower damping capabilities. It is observed that macrocomposites have increased tan δ value than microcomposites. In the case of 30-phr microcomposite (NRM30), the tan δ value decreased to 1.18, which is lower than the

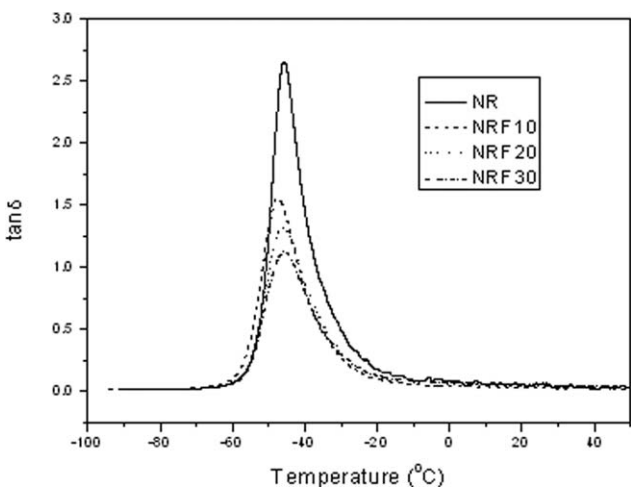

Figure 5 Tan δ vs. temperature curve of untreated oil palm macrofiber/NR composites having various fiber content.

TABLE IV
Peak Height, T_g from tan δ, and Activation Energy of the Composites

Composite	Peak height (tan δ_{max})	tan δ_{max} (T_g)	Activation energy (kJ/mol)
NR	2.65	−46.4	258.24
NRF30	1.19	−45.8	258.12
NRM30	1.18	−45.4	312.84
NRMS30	1.11	−44.01	369.68
NRMH30	1.15	−44.48	350.24

value of the macrofiber-reinforced composite. Also the T_g value shows a slight shift to higher temperatures for 30-phr microfibril composite, which is higher than macrocomposite (Table IV). The reason why alkali-treated microfibril composites have lower tan δ is because of strong and rigid microfibril/rubber interface due to improved adhesion, the molecular mobility in the interfacial zone is reduced. Molecular motion along the rubber macromolecular chain is severely hindered, which results in low damping properties. Therefore, we can conclude that cellulose microfibrils decrease the damping of the composite.

The reason why microfiber-reinforced composites show moderate increase in storage modulus and low tan δ compared with macrocomposites is the strong and rigid fiber/matrix interaction in microcomposites. Thus microfiber-reinforced composites exhibit better dynamic properties than macrocomposites.

Effects of chemical modification on dynamic properties

Storage modulus

The dynamic mechanical properties of composites are very much influenced by the chemical treatment given to the microfibril surface. The effect of chemical treatments on the storage modulus of microfibril-reinforced composite is given in Figure 8. It is clear that an improvement in the storage modulus is observed for chemically treated microcomposites, which is due to the increase in the interfacial stiffness achieved through more intense microfibril–matrix interaction, that is, there exists a better interfacial adhesion between the fibril and matrix. As seen in the figure, maximum storage modulus is shown by the composite in which fibrils are treated with silane coupling agent (NRMS30), followed by treatment with benzoyl chloride (NRMB30) and then with resorcinol-silica bonding system (NRMH30). The increase in adhesion in silane-treated microcomposite is attributed to the decreased hydrophilic nature of treated fibrils, which improves the interaction with the hydrophobic NR matrix. The hydrolyzed silanols form strong covalent bond or hydrogen bond with —OH functional group of cellulose. The individual coupling agent molecules attached to cellulose microfibrils form a continuous network structure. In addition, the treated surface was very rough and had a number of voids that provides better mechanical interlocking with the NR matrix. The coupling and bonding agents increase the fibril/matrix adhesion, causing lesser molecular mobility in the interfacial region. Because the fibrils are well dispersed in the matrix, formation of more crosslinks between fibril network and rubber matrix is possible, leading to a stiffer composite. For the alkali-treated composite, the moisture absorbing capacity of fibrils is reduced, leading to improved wetting, which in turn produces a strong interfacial bond with the rubber matrix and gives rise to a stiffer composite with high E' values. In the case of benzoylated fibril composites, the improvement in interfacial adhesion is attributed to the presence of phenyl structure, which enhances bonding between fibril surface and NR matrix. The

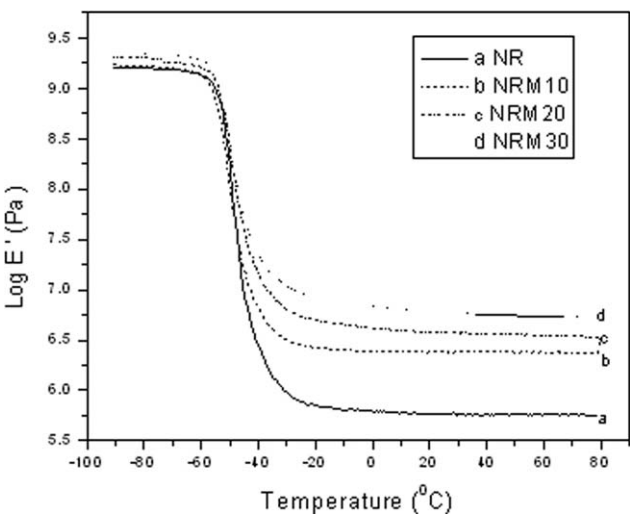

Figure 6 Storage modulus vs. temperature curve of oil palm microfiber/NR composites having various fiber content.

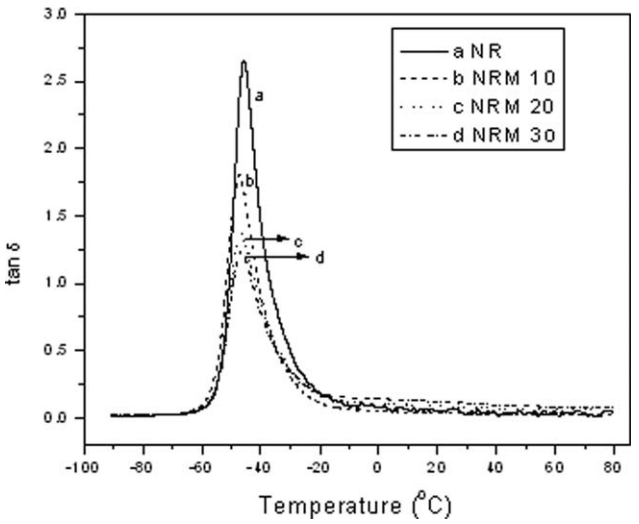

Figure 7 Tan δ vs. temperature curve of oil palm microfiber/NR composites having various fiber content.

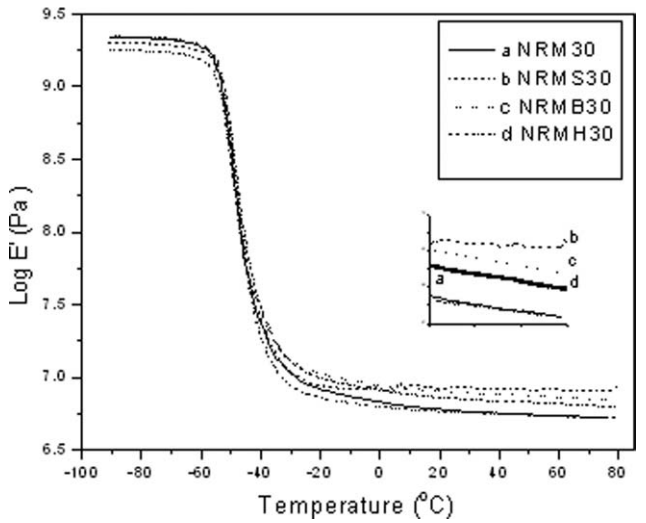

Figure 8 Storage modulus vs. temperature curve of treated oil palm microfiber/NR composites.

reduction in hydrophilic nature makes the fibril more compatible with hydrophobic NR and the rough surface improves the mechanical interlocking of the NR molecules with the fibrils and shows better fiber matrix adhesion.

The effectiveness of fillers on the moduli of the composites can be represented by a coefficient *C* such as[27]

$$C = (E'_g/E'_r)_{\text{comp}}/(E'_g/E'_r)_{\text{gum}} \quad (1)$$

where E'_g and E'_r are the storage modulus values in glassy and rubbery region. The higher the values of *C*, the lower will be the effectiveness of the filler. The values of coefficient *C* are given in Table V. From the table, we can infer that the composite NRMS30, in which microfibrils are silane treated and has lower coefficient *C* value, shows better fiber matrix interaction. We can conclude that chemical treatment increases the storage modulus values of microcomposites.

Damping factor

The variation of tan δ of treated microfibril-reinforced composites with temperature is given in Figure 9. Here the chemically treated microfibril composites have decreased damping characteristics than the macrofiber-reinforced composites. The tan δ peak height of silane-treated composite (NRMS30) is lower than the value of untreated microcomposite NRM30. Among the treated composites the height of tan δ peak is almost same for all the composites (Table IV). The T_g value of treated microfibril composites shifts slightly to higher temperatures when compared with untreated microcomposites. The reason why treated microcomposites possess low tan δ is because of strong reinforcement of the matrix by the addition of

TABLE V
The Value of the Constant *C*

Composite	Coefficient *C*
NRF30	0.88
NRM30	0.87
NRMS30	0.83
NRMB30	0.85
NRMH30	0.86

treated fibrils that are well bonded to the rubber matrix. As a consequence, molecular motion along the rubber macromolecular chain is severely hindered leading to low tan δ values. Hence, treated microfibrils decrease the damping of the composites.

Treated microfiber-reinforced rubber composites show higher storage modulus compared with untreated ones because of increased crosslinking and formation of strong fiber/matrix interface. The damping properties of the treated composites were found to decrease with chemical modification. Therefore, we can conclude that treated microfibrils-reinforced composites exhibit better dynamic properties than untreated ones.

The SEM images of tensile fracture surfaces of untreated and treated microcomposites are shown in Figure 10(a,b), respectively. In the untreated composites, (a) the bonding between rubber matrix and fiber is weak and hence it shows the presence of holes, indicating easy fiber pull out, which has taken place because of poor wetting. In the case of the composite containing microfibrils treated with silane coupling agent, (b) the moisture content of the fibrils was greatly reduced. Because of high aspect ratio and surface area of microfibrils, stronger bonding between fibrils and matrix will take place. This is evident from the short broken fibril ends that can be seen in the micrograph. Thus SEM studies further

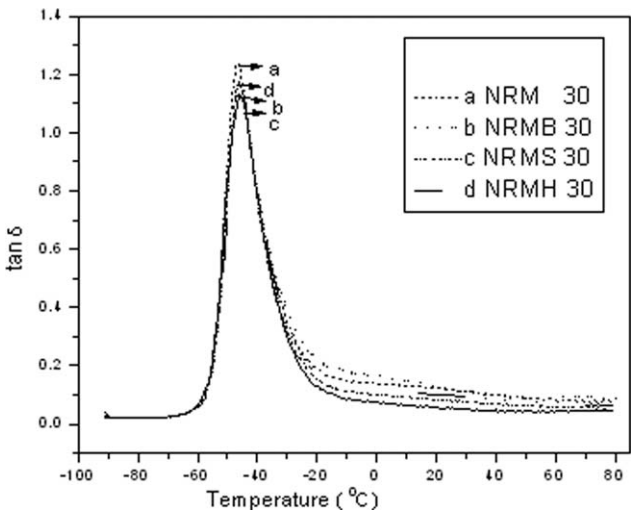

Figure 9 Tan δ vs. temperature curve of treated oil palm microfiber/NR composites.

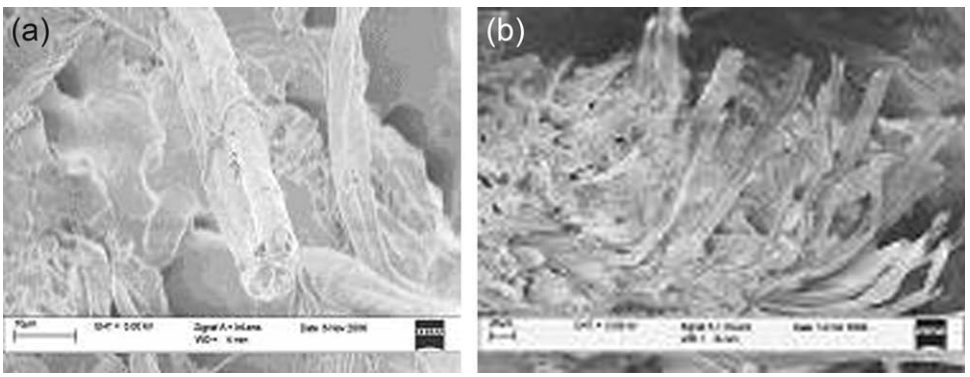

Figure 10 SEM images of the tensile fracture surface of (a) untreated microfiber composite, showing fiber matrix debonding and fiber pull out, and (b) silane-treated microfiber composite, showing good fibril–matrix adhesion.

support the indication of better adhesion by chemical treatment of cellulose microfibrils.

Effect of frequency

The storage modulus and damping peaks were affected by frequency. The variation of E' and tan δ with temperature at three different frequencies 0.1, 1 and 10 Hz of silane-treated composite is shown in Figures 11 and 12, respectively. If a compound is subjected to a constant stress, its elastic modulus is expected to decrease with time because of the molecular rearrangement, to minimize the localized stress. Therefore, as the frequency increases there is an increase in E' values. The modulus values were found to be decreased as temperature increases from –70 to –40°C. It can be observed that there was an increase in storage modulus with increase in frequency and this increase is prominent only at low temperatures. This phenomenon may be due to the lesser mobility of the rubber chains when the speed of the cyclic stress is too fast to bring about deformation. The molecules will not get time to undergo permanent deformation (irreversible flow) and so the material exhibits elastic behavior, resulting in an increase of E' values. The tan δ peak is found to shift to higher temperature with increase of the frequency. The damping peak is associated with the partial loosening of the polymer structure so that groups and small chain segments can move. The tan δ peak, which is indicative of the glass transition temperature, is also indicative of the degree of crosslinking of the system. Increase of frequency is found to have a broadening effect on the tan δ curve. The broadening of the curve is due to some kind of heterogeneity in the network structure.

Activation energy for glass transition

The glass transition temperatures of NR composites obtained from tan δ are given in Table IV. The table shows that the T_g values of composites are lower than the gum compound. Akay[28] reported that the T_g values obtained from the loss modulus were more realistic than those obtained from damping factor. The activation energy, ΔE, for the glass

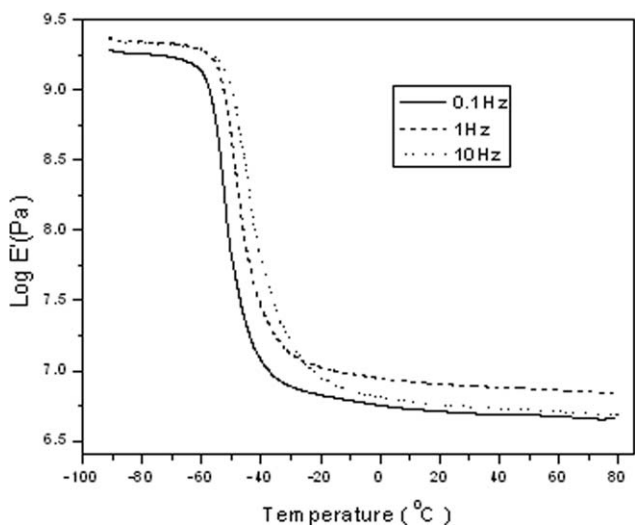

Figure 11 Effect of frequency on E' of silane-treated oil palm microfiber/NR composites.

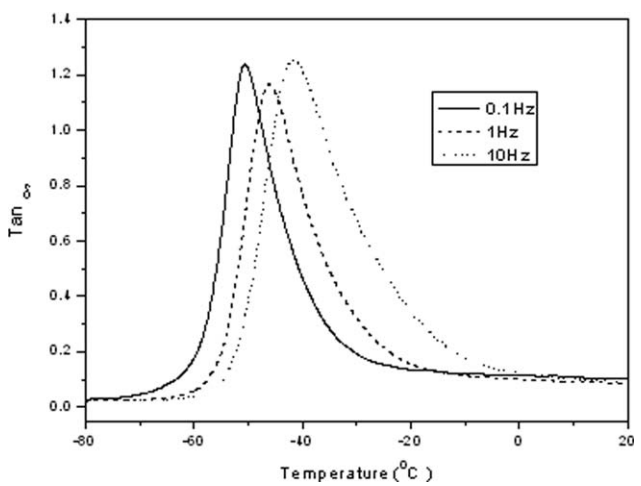

Figure 12 Effect of frequency on tan δ of silane-treated oil palm microfiber/NR composites.

TABLE VI
Experimental and Theoretical Storage Moduli Value at 0.1 Hz for Different Loadings

Composite	Storage modulus ($\times 10^8$ Pa)			
	Experimental value	Equation (3)	Equation (4)	Equation (5)
NR	8.825	8.825	8.825	8.825
NRM10	8.985	8.771	8.482	8.938
NRM20	9.116	8.824	8.752	9.421
NRM30	9.425	8.675	8.461	9.579

transition of the composite can be calculated from the Arrhenius equation:

$$f = f_0 \exp^{(-\Delta E/RT)} \quad (2)$$

where f is the measuring frequency, f_0 is the frequency when T approaches infinity, and T is the temperature corresponding to the maximum of tan δ curve. Table IV gives the activation energy values for the glass transition of NR composites. Among the composites, activation energy is highest for silane-treated microfibril composite, indicating better fibril/matrix adhesion and stiffness of the composites.

Theoretical prediction of storage modulus

The simplest equation for the reinforcement of a material due to an inclusion was given by Einstein.[29] The equation is given as

$$E_c = E_m(1 + 1.25V_f) \quad (3)$$

where E is the storage modulus, subscripts c and m represent composite and matrix, and V_f is the volume fraction of fiber.

Another equation proposed by Einstein was

$$E_c = E_m(1 + V_f) \quad (4)$$

where the terms are the same as explained earlier.

The Einstein's theory was modified by Guth.[30] The equation proposed is

$$E_c = E_m(1 + 2.5V_f + 14.1V_f^2) \quad (5)$$

The experimental and theoretical storage moduli values at 0.1 Hz for varying microfibril loading are given in Table VI. It can be seen from the table that at 10% fibril loading, Einstein's equations show slight negative deviation from the experimental values, and Guth equation agree with the experimental values. At 10-phr fibril loading, Einstein's model deviate from the experimental values by 6.8–7.93%, whereas at 20% loading they deviate by 6.3–8.89%. Thus, we can conclude that Einstein's models approximate the experimental data in the same manner at both microfibril loading.

When the amount of microfibril is increased to 30 phr, Guth model agree the best, but Einstein's equations show deviations from the experimental values. In the case of macrocomposite, both models show slight deviations. The matrix/fiber interaction is weaker in the case of macrocomposite. The fiber agglomeration during processing and low aspect ratio of macrofibers is not considered in the equations. In the case of microcomposite, Guth model considered the strong interfacial adhesion between the matrix and microfibrils. The stiffness of the composite increases and this factor is also considered in Guth model.

CONCLUSION

The dynamic mechanical properties of NR reinforced with macro/microfibrils of oil palm fiber have been investigated. The storage modulus of the composites was found to increase with fiber loading because of the reinforcement imparted by the fillers. The unfilled compound has the highest tan δ value, indicating a large degree of mobility and hence good damping characteristics. Addition of macro/microfibers decreased the damping characteristics of composites, as the fibers acted as barriers to the free movement of the macromolecular chain. Incorporation of treated microfibrils resulted in higher storage modulus, because of increased silane coupling crosslinking and formation of a strong fibril/matrix interface. The composites containing microfibrils treated with silane coupling agent showed maximum dynamic properties. The glass transition shifted to the positive side on the addition of treated microfibers. It was found that the incorporation of treated microfibrils decreased the damping characteristics of the composite as the fibers acted as barriers to the free movement of the macromolecular chain. Increase of frequency is found to have a broadening effect on the tan δ curve. Activation energy for the glass transition of neat NR and the composites was calculated and found maximum for the treated microfiber-reinforced composites. It is also clear that from cellulose microfibril composites, it is possible to prepare user-friendly and cost-effective composite materials possessing appropriate stiffness and damping behavior. This composite will be a suitable substitute for conventional structural materials in engineering applications.

References

1. Malunka, M. E.; Luyt, A. S.; Krump, H. J Appl Polym Sci 2006, 100, 1607.
2. Okieimen, F. E.; Imanah, J. E. J Appl Polym Sci 2006, 100, 2561.

3. Suhara, P. P.; Mohini, S. Compos Part A: Appl Sci Manuf 2007, 38, 1445.
4. Mohanty, A. K.; Misra, M.; Drazal, L. T. J Polym Environ 2002, 10, 19.
5. Helene, A.; Sonia, M. B.; Dufresne, A. Macromol Symp 2006, 233, 132.
6. Gwanghoon, K.; Pillsung, K.; Shin, H.; Seunghwon, L.; Hyungkyu, C.; Sunhyun, K. J Appl Polym Sci 2007, 105, 477.
7. Aprem, A. S.; Joseph, K.; Thomas, S. J Appl Polym Sci 2004, 91, 1068.
8. Rana, A. K.; Mandal, A.; Bandyopadhyay, B. Compos Sci Technol 2003, 63, 801.
9. Wanvimon, A.; Nuchanat, N.; Garry, L. R. J Appl Polym Sci 2005, 98, 34.
10. Amash, A.; Zugenmaier, P. Polymer 2000, 41, 1589.
11. Joseph, P. V.; Mathew, G.; Joseph, K.; Groenincks, G.; Thomas, S. Compos Part A: Appl Sci Manuf 2003, 34, 275.
12. Idikula, M.; Malhotra, S.; Joseph, K.; Thomas, S. J Appl Polym Sci 2005, 97, 2168.
13. Jacob, M.; Francis, B.; Thomas, S.; Varghese, K. T. Polym Compos 2006, 27, 671.
14. Geethamma, V. G.; Kalaprasad, G.; Gabriel, G. G.; Thomas, S. Compos Part A: Appl Sci Manuf 2006, 36, 1499.
15. Jong, L. Compos Part A: Appl Sci Manuf 2006, 37, 438.
16. Haghighat, M.; Zadhoush, A.; Nourikhorasani, S. J Appl Polym Sci 2005, 96, 2203.
17. Martins, M. A.; Mattoso, L. H. C. J Appl Polym Sci 2004, 91, 670.
18. Menon, A. R. R.; Sonia, T. A.; Sudha, J. D. J Appl Polym Sci 2006, 102, 4801.
19. Kosikova, B.; Osvald, A.; Krajcovicova, J. J Appl Polym Sci 2007, 103, 1226.
20. Da Costa, H. M.; Visconte, L. L. Y.; Nunes, R. C. R.; Furtado, C. R. G. J Appl Polym Sci 2002, 83, 2331.
21. Sepe, M. P. Dynamic Mechanical Analysis for Plastics; Plastic Design Library: New York, 1998.
22. Guo, W.; Ashida, M. J Appl Polym Sci 1993, 50, 1435.
23. Joseph, K.; Thomas, S.; Pavithran, C. J Reinforc Plast Compos 1993, 12, 139.
24. Dufresne, A.; Cavaille, J. Y.; Helbert, W. Macromolecules 1996, 29, 7624.
25. Agnes, F.; Martins, L. L.; Visconte, Y.; Nunes, R. C. R. J Appl Polym Sci 2005, 97, 2125.
26. Varghese, S.; Kuriakose, B.; Thomas, S. J Adhes Sci Technol 1994, 8, 234.
27. Tan, J. K.; Kitano, T.; Hatakeyama, T. J. Mater Sci 1990, 25, 3380.
28. Akay, M. Comp Sci Technol 1993, 47, 419.
29. Einstein, A. Investigations on the Theory of Brownian Movement; Dover: New York, 1956.
30. Guth, E. J Appl Phys 1951, 22, 16.